Translational Oncology
www.transonc.com

Volume 4 Number 4 August 2011 pp. 241–248 241

Glucose Metabolism Measured by [18F]Fluorodeoxyglucose Positron Emission Tomography Is Independent of PTEN/AKT Status in Human Colon Carcinoma Cells[1]

Quang-Dé Nguyen*, Meg Perumal*, Todd A. Waldman† and Eric O. Aboagye*

*Comprehensive Cancer Imaging Centre, Department of Surgery and Cancer, Imperial College London Faculty of Medicine, Hammersmith Hospital, London, UK; †Lombardi Comprehensive Cancer Center, Department of Oncology, Georgetown University School of Medicine, Washington, DC, USA

Abstract

The phosphoinositide 3-kinase (PI3K) signaling pathway is one of the most altered in cancer, leading to a range of cellular responses including enhanced proliferation, survival, and metabolism, and is thus an attractive target for anticancer drug development. Stimulation of the PI3K pathway can be initiated by alterations at different levels of the signaling cascade including growth factor receptor activation, as well as mutations in *PIK3CA*, *PTEN*, and *AKT* genes frequently found in a broad range of cancers. Given its role in glucose metabolism, we investigated the utility of [18F]fluorodeoxyglucose positron emission tomography ([18F]FDG PET) as a pharmacodynamic biomarker of PI3K pathway–induced glucose metabolism. *PTEN* deletion in human colon carcinoma cells led to constitutive AKT activation but did not confer a phenotype of increased cell proliferation or glucose metabolism advantage *in vivo* relative to isogenic tumors derived from cells with a wild-type allele. This was not due to the activation context, that is, phosphatase activity, *per se* because *PIK3CA* activation in xenografts derived from the same lineage failed to increase glucose metabolism. Acute inhibition of PI3K activity by LY294002, and hence decreased activated AKT expression, led to a significant reduction in tumor [18F]FDG uptake that could be explained at least in part by decreased membrane glucose transporter 1 expression. The pharmacodynamic effect was again independent of *PTEN* status. In conclusion, [18F]FDG PET is a promising pharmacodynamic biomarker of PI3K pathway inhibition; however, its utility to detect glucose metabolism is not directly linked to the magnitude of activated AKT protein expression.

Translational Oncology (2011) 4, 241–248

Introduction

The phosphoinositide 3-kinase (PI3K) signaling pathway is one of the most altered in cancer, initiating direct downstream activation of the serine-threonine kinase AKT, which is vital to the growth and survival of cancer cells [1]. As a major downstream effector of receptor tyrosine kinases and G protein–coupled receptors, PI3K transduces signals from various growth factors and cytokines into intracellular messages by converting phosphatidylinositol-4,5-biphosphate (PIP2) to phosphatidylinositol-3,4,5-triphosphate (PIP3) at the membrane, providing docking sites for signaling proteins containing pleckstrin homology domains, including 3-phosphoinositide–dependent kinase 1 and serine-threonine kinase AKT. While colocated at the membrane, 3-phosphoinositide–dependent kinase 1 phosphorylates and activates AKT, which elicits a wide range of downstream signaling events. The tumor suppressor *PTEN* (phosphatase and tensin homolog) is the most important negative regulator of the PI3K signaling pathway by

Address all correspondence to: Eric O. Aboagye, PhD, Comprehensive Cancer Imaging Centre, Department of Surgery and Cancer, Imperial College London Faculty of Medicine, Hammersmith Hospital, Du Cane Road, London W12 0NN, UK.
E-mail: eric.aboagye@imperial.ac.uk

[1]This work was funded by Cancer Research UK–Engineering and Physical Sciences Research Council grant C2536/A10337. E.O.A.'s laboratory receives core funding from the UK Medical Research Council (U1200.005.00001.01).
Received 11 February 2011; Revised 15 March 2011; Accepted 15 March 2011

DOI 10.1593/tlo.11118

functionally antagonizing PI3K activity through its intrinsic lipid phosphatase activity that converts PIP3 back to PIP2, therefore reducing the cellular pool of PIP3 [2]. Recent human cancer genome studies have revealed that many components of the PI3K pathway, including the *PIK3CA* gene coding for the p110 catalytic subunit of PI3K, and the *PTEN* and *AKT* genes, are frequently mutated (germ line or somatic mutations) in a broad range of human cancers. The *PTEN* gene was initially identified as a tumor suppressor candidate in 1997 [3,4]. Numerous mutations and/or deletions in the *PTEN* gene have been found in human cancer cell lines and tumor tissues, indicating a strong association between loss of *PTEN* function and human cancer [2,5]. In addition, germ line mutations in the *PTEN* gene have been associated with Cowden syndrome and related diseases in which patients experience a significantly increased risk of certain tumors, including breast and thyroid carcinomas. Most *PTEN*-related studies have focused on its tumor suppressor function, and an accumulating body of evidence supports the notion that impaired *PTEN* function induces PIP3 accumulation and subsequent AKT hyperactivation, leading to oncogenic transformation of cells [6]. These findings, and the fact that PI3K and other downstream kinases are amenable to pharmacological intervention, make this pathway one of the most attractive therapeutic targets in cancer [7,8].

Given the large number of PI3K pathway therapeutics in development, introduction of effective biomarkers that report on target inhibition or drug efficacy will benefit the various drug development strategies. Although molecular pharmacological biomarkers of the PI3K pathway based on immunohistochemical analyses of tissue biopsy samples with phosphospecific antibodies of AKT are available, these techniques have a number of limitations: routine immunohistochemistry is largely qualitative, the location of the neoplastic tissue may prevent the use of invasive procedures, and intratumoral molecular and cellular heterogeneity may significantly confound analyses [9]. In this context, the development of noninvasive imaging strategies to predict and evaluate the activity of PI3K pathway inhibitors in patients would be highly valuable. In the present study, we investigated the potential utility of positron emission tomography (PET) imaging to characterize PI3K signaling pathway activation status in tumor and response to PI3K pathway targeting therapeutics.

The PI3K/AKT signaling pathway has notably been shown to stimulate increased glucose uptake and metabolism in response to growth factors through the increased transcription and plasma membrane localization of the glucose transporter 1 (GLUT-1) [10], the principal glucose transporter expressed in most cell types. The pathway also regulates glycolysis by promoting hexokinase localization to mitochondria and, consequently, glucose phosphorylation, as well as expression of other glycolytic genes through activation of hypoxia-inducible factor 1 [11–17]. This suggests that PET imaging with the glucose analog [^{18}F]fluorodeoxyglucose ([^{18}F]FDG) could be useful as a pharmacodynamic biomarker to probe biologic consequences of the various oncogenic alterations leading to the PI3K pathway activation and, by extension, the response of tumors to PI3K pathway targeting therapeutics.

In an effort to better understand the contribution of *PTEN* deletion and subsequent AKT hyperactivation to glucose metabolism *in vivo*, we investigated the dynamics of [^{18}F]FDG uptake (and proliferation with [^{18}F]fluorothymidine ([^{18}F]FLT)) in isogenic human colon carcinoma cells that differed only in their *PTEN* status. We also investigated the potential utility of [^{18}F]FDG PET for monitoring PI3K inhibition, in relation with the *PTEN* expression.

Materials and Methods

Cell Culture and Reagents

The isogenic human colon carcinoma set of cells HCT116 PTEN WT/KO and PIK3CA WT/MUT were kindly provided by Dr Todd Waldman and Pr Bert Vogelstein, respectively, and maintained as previously described [18,19]. Insulin and LY294002 were purchased from Sigma-Aldrich (Sigma-Aldrich Company Ltd, Dorset, United Kingdom) and Calbiochem (Merck Chemicals Ltd, Nottingham, United Kingdom), respectively.

Western Blot Analysis

HCT116 PTEN cells were cultured in six-well plates with complete or serum-free growth medium (overnight incubation) and stimulated with insulin at the indicated concentrations for 1 hour. Protein samples were subsequently prepared by lysing cells in RIPA buffer (Invitrogen Ltd, Paisley, United Kingdom) supplemented with protease and phosphatase inhibitor cocktails (Sigma-Aldrich). Tumor tissue samples were obtained as follows. Excised and snap-frozen xenografts were homogenized in RIPA lysis buffer with the PreCellys 24 homogenizer and CK14 beads-containing tubes (two cycles of 25 sec/6500 rpm; Bertin Technologies, Montigny-Le-Bretonneux, France). Equal amounts of protein (30 μg) were denaturated in sample buffer, subjected to SDS–polyacrylamide gel electrophoresis on 4% to 12% gels (Invitrogen Ltd), and transferred to polyvinylidene fluoride membranes (GE Healthcare Life Sciences, Buckinghamshire, United Kingdom). The membranes were immunoblotted with specific primary antibodies, horseradish peroxidase–conjugated secondary antibodies, and visualized by enhanced chemiluminescence (GE Healthcare Life Sciences). The following antibodies were used: anti–phospho-AKT (Ser473) and anti–AKT rabbit polyclonal antibodies (Cell Signaling Technology, Inc, Danvers, MA), a mouse monoclonal anti–PTEN antibody (Cascade Bioscience, Winchester, MA), a mouse monoclonal anti–α-tubulin antibody (Santa Cruz Biotechnology, Inc, Santa Cruz, CA), and secondary goat antimouse and antirabbit horseradish peroxidase antibodies (Santa Cruz Biotechnology).

Proliferation Assay

Assessment of *in vitro* cell proliferation was performed using the colorimetric 3-(4,5-dimethylthiazol-2-yl)-2,5-diphenyltetrazolium bromide MTT assay according to manufacturer's instructions (ATCC, Manassas, VA). Briefly, HCT116 PTEN cells were seeded in triplicate in 96-well plates with complete or serum-free growth medium in the absence or presence of PI3K inhibitor LY294002 (overnight incubation) and stimulated with insulin at the indicated concentrations. Cell proliferation was quantified the next day by adding 10 μl of MTT per well and recording the absorbance at 570 nm.

[^{18}F]FLT and [^{18}F]FDG Small-Animal PET Imaging

The *in vivo* experimental xenograft model was established by subcutaneous injection of 1×10^6 HCT116 PTEN and PIK3CA isogenic cells on the flanks of 6- to 8-week-old female BALB/c nude mice (Harlan, Wyton, United Kingdom), bilateral implants for each pair of isogenic cells, that is, on the left and right flanks of the same animal. All animal experiments were done by licensed investigators in accordance with the UK Home Office Guidance on the Operation of

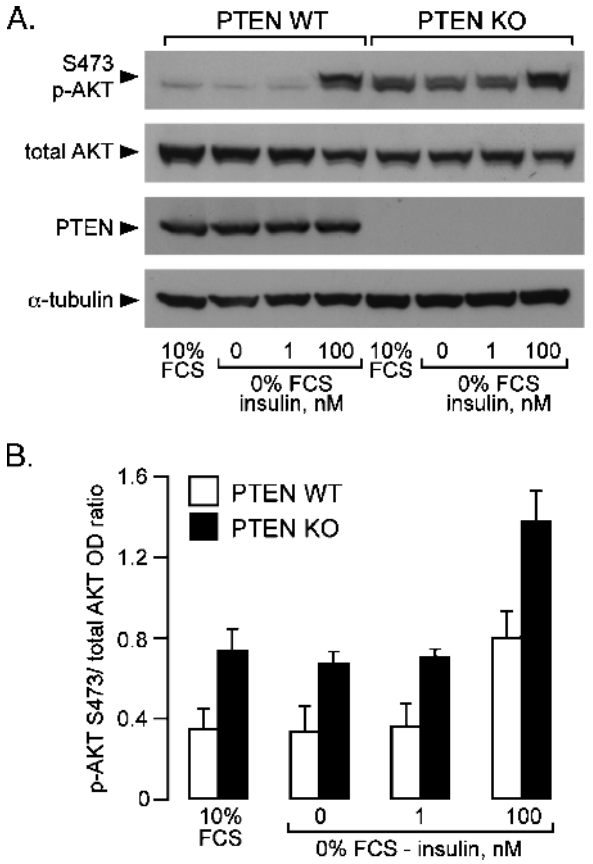

Figure 1. Constitutive AKT activation and insulin-induced AKT hyperactivation in HCT116 PTEN-deleted cells. (A) HCT116 PTEN WT and KO cells were cultured overnight in the absence (0%) or presence (10%) of fetal calf serum (FCS), and then stimulated with insulin (1 or 100 nM) or corresponding vehicle for 1 hour. Protein lysates were prepared, and immunoblots were performed with the indicated primary antibodies. α-Tubulin was used as a loading control. (B) Densitometry (optical density, OD) measurements of phospho-AKT/total AKT ratio extracted from the protein immunoblots. Data represent the mean ± SEM of three to five independent experiments.

the Animal (Scientific Procedures) Act 1986 (HMSO, London, United Kingdom, 1990) and within guidelines set out by the UK National Cancer Research Institute Committee on Welfare of Animals in Cancer Research [20]. When xenografts reached ~100 mm^3, mice were injected twice with LY294002 (100 mg/kg intraperitoneally) or vehicle (10% dimethyl sulfoxide/phosphate-buffered saline) at 3 hours 30 minutes before PET scanning. Imaging was performed on a dedicated small-animal PET scanner (quad-HIDAC; Oxford Positron Systems, Weston-on-the-Green, United Kingdom). Anesthetized animals were placed within a thermostatically controlled bed and positioned prone within the scanner. The bed was calibrated to provide a mouse rectal temperature of ~37°C. A bolus injection of [18F]FLT or [18F]FDG (~3.7 MBq) was given intravenously through the tail vein cannula, and scanning commenced. Dynamic emission scans were acquired in list-mode format for 60 minutes. The acquired data were then sorted into 0.5-mm sinogram bins and 19 time frames (0.5 × 0.5 × 0.5-mm voxels; 4 × 15, 4 × 60, and 11 × 300 seconds) for image reconstruction, which was done by filtered back projection using a two-dimensional Hamming filter (cutoff, 0.6). The image data sets obtained were transferred to a SUN workstation (Ultra 10; SUN Microsystems, Santa Clara, CA) and visualized using the Analyze software (version 6.0; Biomedical Imaging Resource, Mayo Clinic, Rochester, MN). Cumulative images of the dynamic data obtained 30 to 60 minutes (for tumor or liver) or 0 to 1 minutes (for heart) after radiotracer injection were used to visualize radiotracer uptake and to define the regions of interest. Count densities from at least five adjacent planes were averaged for each region of interest at each of the 19 time points to obtain time-*versus*-radioactivity curves (TACs). Tumor TACs were normalized to those of heart or liver at each of the time points to obtain the normalized uptake value (NUV). The NUV at 60 minutes after injection (NUV_{60}), the area-under-the-NUV curve (AUC) calculated as the integral of NUV from 0 to 60 minutes, and the fractional retention of tracer (FRT), the radioactivity at 60 minutes relative to that at 2.5 minutes, were used for comparisons. FRT is a useful variable in that it indicates the proportion of radiotracer delivered to the tumor that is retained. It therefore normalizes tumor tracer uptake to delivery.

GLUT-1 Immunohistochemistry Assay

After PET imaging studies, tumor tissues were excised, fixed in formalin, embedded in paraffin, sectioned (5-μm slices), and processed for GLUT-1 fluorescent immunodetection using the anti–GLUT-1 polyclonal antibody (Abcam, Cambridge, MA) coupled with the Alexa Fluor 488 goat antirabbit (Invitrogen Ltd). The ProLong Gold Antifade mounting solution (Invitrogen Ltd) containing 4′,6-diamidino-2-phenylindole was added to tissue sections before mounting in coverslips, and images were captured using an Olympus BX51 fluorescent microscope (Olympus Ltd, Southall, United Kingdom).

Statistical Analysis

Data were expressed as mean ± SEM, and the significance of comparison between two data sets was determined using Student's *t* test (GraphPad Prism, version 5.0a for Macintosh; GraphPad, San Diego,

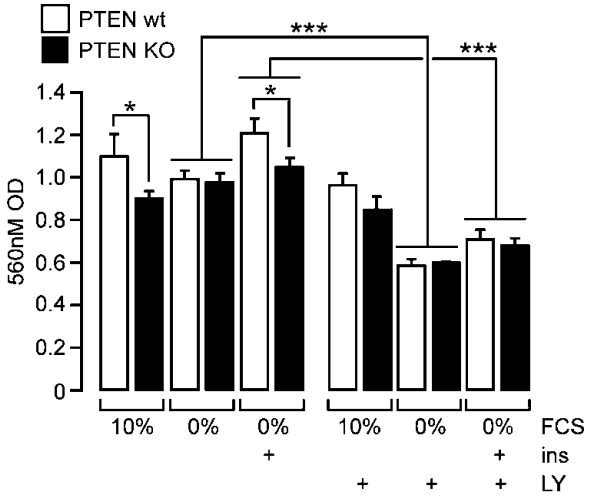

Figure 2. *In vitro* assessment of proliferation related to PTEN status and LY294002 treatment. HCT116 PTEN WT and KO cells were cultured in the absence (0%) or presence (10%) of fetal calf serum (FCS) and LY294002 (LY, 10 μM), and stimulated with insulin (ins, 1 or 100 nM) or corresponding vehicle overnight. Cell proliferation was assessed after 24 hours. Data represent the mean ± SEM of three to five independent experiments performed in triplicate.

CA) and defined as significant (*.01 < P < .05), very significant (**.001 < P < .01), and extremely significant (***P < .001).

Results

Effect of PTEN *Deletion on AKT Status in Unstimulated and Serum/Growth Factor–Stimulated Cancer Cells*

We investigated the biologic impact of *PTEN* deletion on AKT status using an isogenic set of human colon carcinoma cells that differ only in the presence or complete absence (through somatic cell gene targeting) of endogenous wild-type *PTEN* expression (HCT116 PTEN WT and HCT116 PTEN KO, respectively) [18]. As expected, HCT116 PTEN KO cells exhibited constitutive AKT activation, as assessed by phosphorylated serine-473 AKT protein cellular content compared with their isogenic counterpart HCT116 PTEN WT. There was approximately two-fold increased p-AKT/total AKT ratio (Figure 1, *A* and *B*). The presence or absence of serum within the growth medium did not affect AKT activation status in both cell lines. Interestingly, stimulation of the cells with 100 nM insulin induced AKT activation in HCT116 PTEN WT cells to levels similar to those in *PTEN*-deleted cells at baseline. Insulin treatment also led to hyperactivation of AKT in HCT116 PTEN KO, with the p-AKT/AKT ratio approximately two-fold higher than that in the untreated PTEN KO cells, suggesting that the *PTEN*-deleted cells display hyperactivated AKT (over the constitutive activated AKT protein level) in response to growth factor stimulation.

PTEN *Deletion/AKT Hyperactivation Is Not Associated with a Growth Advantage*

AKT activation has been reported to stimulate cell cycle progression, survival, and migration through phosphorylation of many physiological substrates [17,21,22]. A study also reported that AKT activation is required for both the cell survival and cell proliferation phenotypes observed in *PTEN*-deleted embryonic stem cells [23]. Control of cell proliferation by PI3K/AKT is not, however, universal. For example, activation of AKT in mammary epithelial carcinoma cells was not associated with an increased tumor growth rate; furthermore, induction of constitutive AKT expression in nontumorigenic human breast epithelial cells had minimal phenotypic consequences and did not recapitulate the biochemical and growth characteristics seen with somatic cell knock-in of *PIK3CA* gene [24–26]. We investigated the impact of *PTEN* deletion on cell proliferation *in vitro* using a colorimetric assay and *in vivo* using [18F]FLT small-animal PET imaging (Figures 2 and 3). Cell proliferation status was comparable in unstimulated HCT116 PTEN KO and PTEN WT cells, whereas on serum or insulin stimulation, *PTEN*-deleted cells exhibited significant lower cell proliferation rates compared with the isogenic cell counterpart (approximately 15%-20% decrease; Figure 2). This result is in line with studies reporting induction of cell growth arrest and cellular senescence in *PTEN*-deleted/AKT-activated human prostate and colon carcinoma cells, through a p53-dependent mechanism [27–29]. The *in vivo* tumor proliferation status of size-matched HCT116 PTEN WT and HCT116 PTEN KO xenografts-bearing mice was assessed by [18F]FLT-PET [9]. The significantly lower [18F]FLT uptake in PTEN KO tumors compared with PTEN WT tumors was seen on the tumor time-*versus*-radioactivity curves and extracted semiquantitative values (approximately 20% lower NUV_{60}; Figure 3). Our *in vitro* and *in vivo* data, therefore, indicated that *PTEN* deletion/AKT constitutive activation in the HCT116 PTEN isogenic set is associated with a decreased cell proliferation rate.

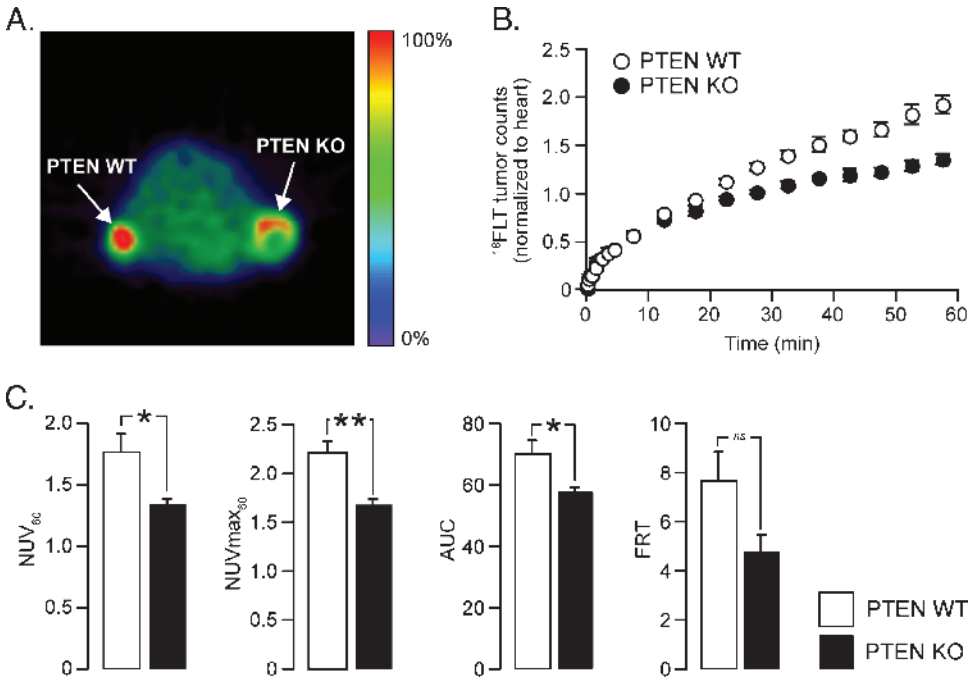

Figure 3. *In vivo* assessment of proliferation related to PTEN status using [18F]FLT PET imaging. Size-matched HCT116 PTEN WT and KO (bilateral implant) xenografts-bearing mice (n = 5) were subjected to 60 minutes of dynamic [18F]FLT PET imaging. (A) [18F]FLT PET image of one representative mouse (arrows indicate the tumors). (B) The tumor time-*versus*-radioactivity curve normalized to heart (TAC). (C) Semiquantitative imaging variables (NUV_{60}, AUC, and FRT) extracted from the TAC. Data are mean ± SEM.

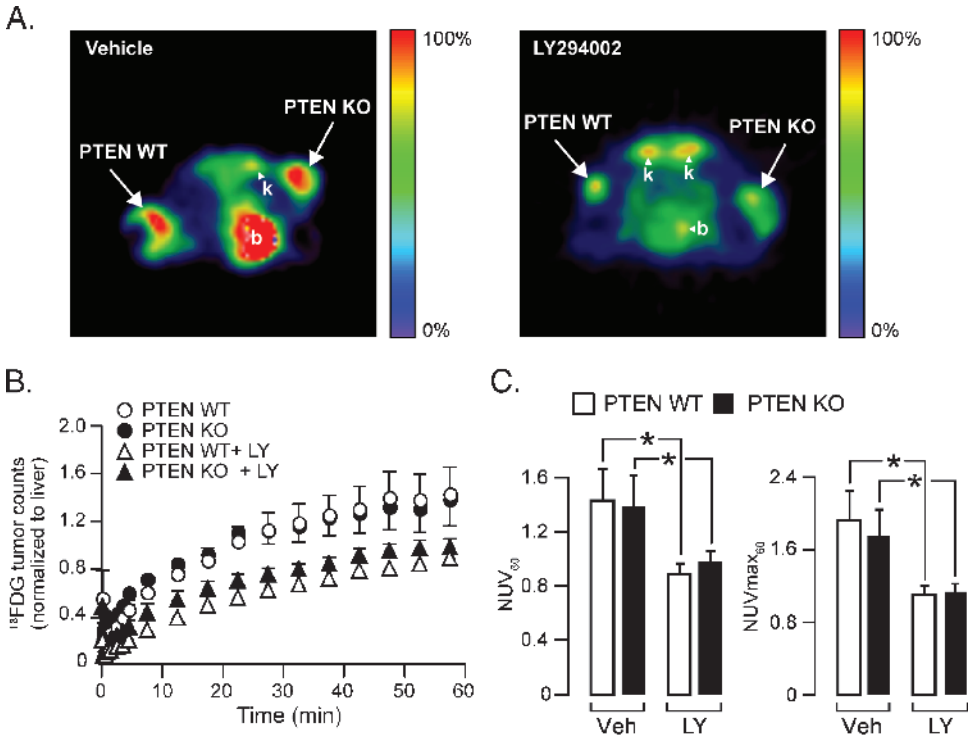

D.

	Vehicle		LY294002	
	PTEN WT	PTEN KO	PTEN WT	PTEN KO
NUV_{60}	1.43 ± 0.23	1.39 ± 0.22	0.89 ± 0.08	0.98 ± 0.07
$NUVmax_{60}$	1.92 ± 0.32	1.75 ± 0.28	1.11 ± 0.08	1.14 ± 0.08
AUC	63.49 ± 8.35	64.16 ± 6.94	36.12 ± 3.74	43.93 ± 3.46
FRT	6.86 ± 1.90	8.13 ± 0.74	4.88 ± 1.41	5.28 ± 0.77

Figure 4. *In vivo* assessment of glucose metabolism related to PTEN status using [^{18}F]FDG PET imaging. HCT116 PTEN WT and KO (bilateral implant) xenografts-bearing mice were treated twice with 100 mg/kg LY294002 (3 hours 30 minutes before imaging, $n = 4$) or corresponding vehicle ($n = 6$) and were subsequently subjected to 60 minutes of dynamic [^{18}F]FDG PET imaging. (A) [^{18}F]FDG PET images of two representative mice (arrows indicate the tumors; b, bladder; k, kidneys). (B) The tumor time-*versus*-radioactivity curve normalized to liver (TAC). (C, D) Semiquantitative imaging variables NUV_{60}, AUC, and FRT extracted from the TAC. Data are mean ± SEM.

PTEN *Deletion/AKT Activation Is Not Associated with a Glucose Metabolism Advantage*

The PI3K pathway regulates glucose uptake and metabolism, and tumors with high levels of PI3K signaling might require high rates of glycolysis for their survival [1,30,31]. Moreover, it has been reported that activation of the PI3K signaling pathway stimulates the switch to aerobic glycolysis characteristic of cancer cells and that AKT activation renders cancer cells addicted to aerobic glycolysis for continued growth and survival [13]. We investigated the dynamics of glucose metabolism of the isogenic HCT116 PTEN WT/KO cells *in vivo* by [^{18}F]FDG PET (Figure 4) and observed equivalent radiotracer uptake kinetics (NUV_{60} = 1.43 ± 0.23 and 1.39 ± 0.22, respectively), indicating that PTEN deletion/AKT constitutive activation was not associated with a glucose metabolic advantage. To demonstrate that this was not due to activation context, that is, phosphatase activity, we conducted a similar [^{18}F]FDG PET imaging study in isogenic HCT116 PIK3CA cells with the parental cells harboring a wild-type PI3K (HCT116 PIK3CA WT) and the isogenic pair cells expressing a constitutively activated PI3K (HCT116 PIK3CA MUT), through targeted homologous integration, as previously described [19]. Similarly, there were no differences in [^{18}F]FDG uptake in HCT116 xenografts derived from PIK3CA WT/MUT cells (Figure 5), supporting our aforementioned assertion that activation of the PI3K pathway detected by p-AKT protein expression *per se* does not directly translate into acquisition of an increased glucose metabolic phenotype.

[^{18}F]FDG PET Imaging Detects Treatment-Induced PI3K Inhibition Independent of PTEN *Status*

Many academic laboratories and pharmaceutical companies are actively developing inhibitors that target PI3K and other key components in the pathway [32]. LY294002 is a small molecule that competitively and reversibly inhibits the ATP binding site of several PI3Ks and has been widely used as a research tool to antagonize PI3K signaling pathway [19,33]. LY294002 was potent *in vitro* in the HCT116 PTEN isogenic cells arresting cell growth by approximately 40% independent of *PTEN* status or insulin stimulation (Figure 2). We, therefore, wondered if acute pharmacological inhibition of PI3K by LY294002 (>3.5 hours) will alter glucose metabolism *in vivo*. LY294002 treatment resulted in approximately 30% decrease

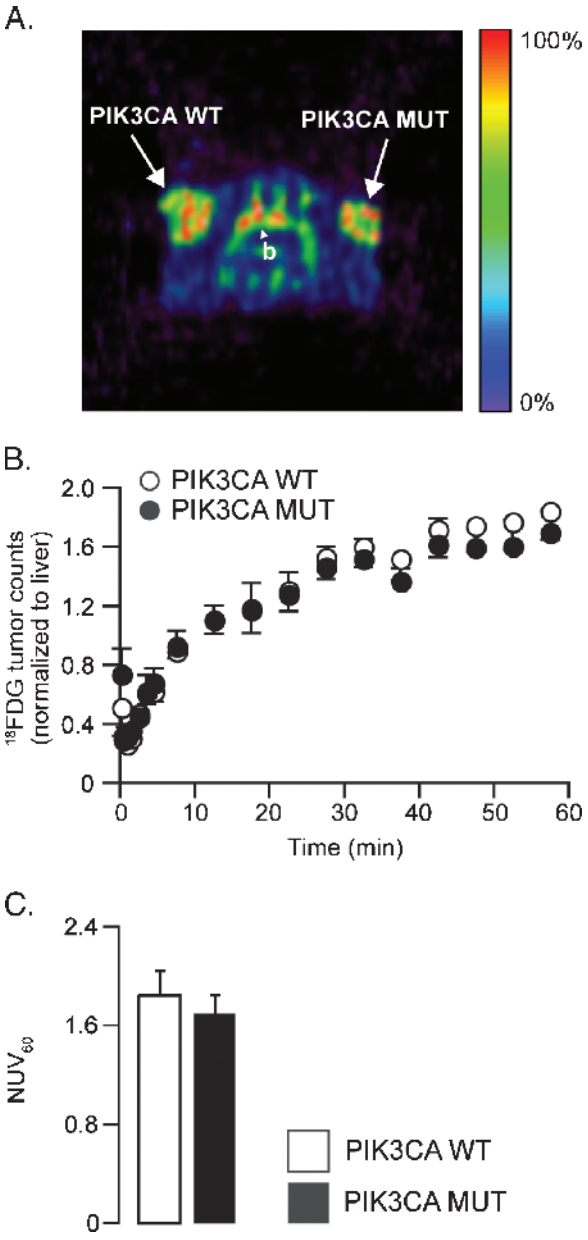

Figure 5. *In vivo* assessment of metabolism related to *PIK3CA* status using [18F]FDG PET imaging. HCT116 PIK3CA WT and MUT (bilateral implant) xenografts-bearing mice ($n = 5$) were subjected to 60 minutes of dynamic [18F]FDG PET imaging. (A) [18F]FDG PET image of one representative mouse (arrows indicate the tumors; b, bladder). (B) The tumor time-*versus*-radioactivity curve normalized to liver (TAC). (C) Semiquantitative imaging variables NUV_{60} extracted from the TAC. Data are mean ± SEM.

in glucose metabolism of the isogenic HCT116 PTEN xenografts, as detected by [18F]FDG PET imaging, independent of their PTEN status (Figure 4). Subsequent *ex vivo* tumor tissues analysis confirmed that PI3K inhibition by LY294002 treatment had resulted in the abrogation of AKT activation conferred by *PTEN* deletion (Figure 6, *A* and *B*), most likely by reducing the PIP3 pool, leading to the redistribution of GLUT-1 from the cell membrane to the cytoplasm, therefore compromising glucose transport and subsequent metabolism (Figure 6*C*).

To summarize, we showed that *PTEN* deletion compared with WT PTEN in the HCT116 isogenic set of cells triggered constitutive activation of AKT and growth factor–dependent AKT hyperactivation, which did not recapitulate the generally described PI3K pathway oncogenic phenotype related to tumor growth and glucose metabolism. Moreover, we showed that the direct inhibition of PI3K resulted in the abrogation of AKT activation, relocation of GLUT-1 to the cytoplasm, and subsequently decreased overall glucose metabolism independent of the PTEN status and that, in our cellular context, [18F]FDG PET imaging could be used as a biomarker of response to anti-PI3K treatment.

Discussion

The loss of PTEN expression or the acquisition of activating PI3K mutations occurs in many tumor types illustrating the importance of the PI3K signaling pathway in cancer. We have shown that the absence of PTEN expression on its own did not confer a proliferation or metabolism advantage as assessed by [18F]FLT and [18F]FDG small-animal PET imaging. Similarly, constitutive PI3K activation alone (*PIK3CA* MUT) was not able to confer an increased glucose metabolic phenotype. Although the contributions of *PTEN* and *PIK3CA* genetic lesions in the PI3K oncogenic signaling pathway are widely reported, the unique implication of each of these components in the overall tumorigenic phenotype of cancer cells is not obvious and might be subjected to a fine balance. A number of studies have found *PTEN*, *PIK3CA*, and *AKT* mutations to be mutually exclusive in individual tumors, suggesting that mutational activation of the PI3K pathway by any one of these means is biologically equivalent [34–36]. These findings are not, however, universal. There are, for instance, reports of a small percentage of tumors with concurrent *PTEN* mutation/deletion and *PIK3CA* mutation [37,38]; the frequency of such events may be higher in particular tumor types and may reflect differences in tumor biology. A recent study also indicates that, in contrast to *PIK3CA* mutations, the *AKT* mutation does not confer growth factor independence and shows distinct phenotypes arising from alterations in the same signaling pathway [26]. AKT hyperactivation alone may, therefore, be insufficient to recapitulate the entire PI3K oncogenic signaling phenotype of increased survival, proliferation, and glucose metabolism. Although p-AKT protein expression was assessed, the direct relationship between the magnitude of protein expression and oncogenic phenotype is unclear. We speculate that protein expression in WT cells is possibly already sufficient to activate glucose metabolism and proliferation. The unexpected reduced proliferation in the HCT116 PTEN KO isogenic cells and xenografts may be due to activation of senescence, analogous to recent report of increased senescence after transgenic expression of activated AKT [39]. Similar to *PTEN* loss, enforced AKT activation leads to senescence that is p53 dependent [27] or p27 dependent [29]. Tumors may adapt to individual *PTEN* or *PIK3CA* genetic changes by a variety of mechanisms. We have only assessed the impact of PTEN on glucose metabolism and proliferation in this present study. The PI3K signaling pathway is also implicated in various oncogenic processes including survival, invasion, and angiogenesis, and further studies will be needed to fully understand the particular role of *PTEN* or *PIK3CA* genetic lesions in the overall tumorigenic phenotype. This will ultimately be highly valuable in the development of imaging biomarkers to fully characterize the efficacy of PI3K pathway targeting therapeutics.

We demonstrated the utility of [18F]FDG PET imaging for the assessment of acute PI3K inhibition and reduced AKT activation

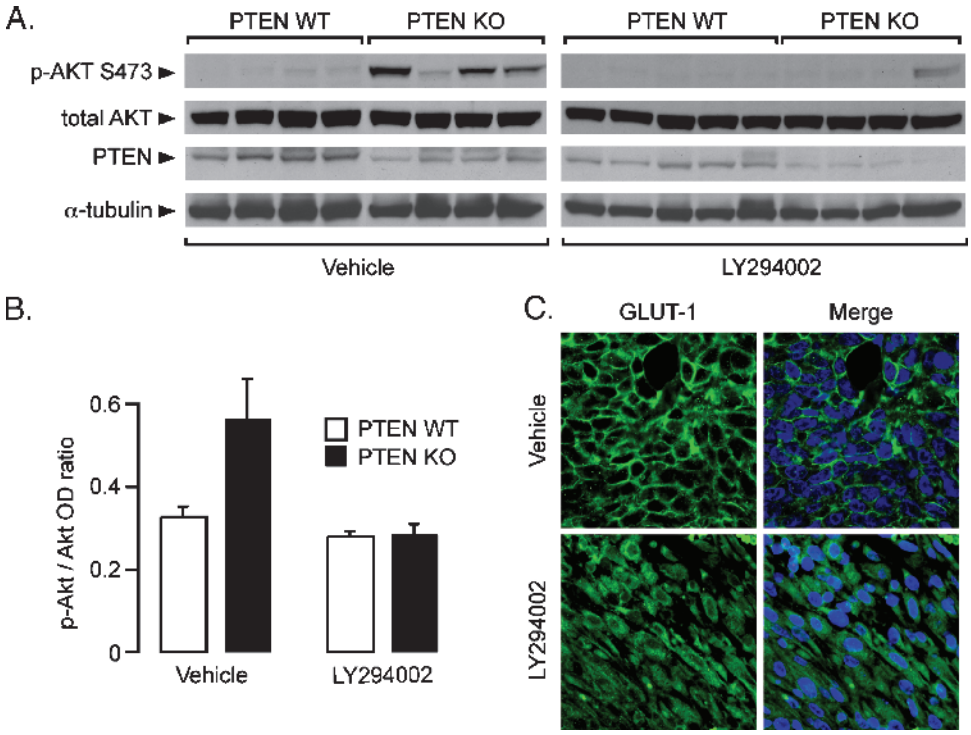

Figure 6. *Ex vivo* assessment of AKT activation status in tumors. (A) Tumor tissues were excised after PET imaging and processed for serine 473 phospho-AKT, total AKT, PTEN, and α-tubulin (loading control). (B) Densitometry (optical density, OD) measurements of phospho-AKT/total AKT ratio extracted from the protein immunoblots. Data represent the mean ± SEM (n = 4-5 tumor tissue). (C) Immunohistochemistry analysis of tumor GLUT-1 cellular localization. Tumor tissues were excised after PET imaging and stained for GLUT-1 (green) and nucleus (4′,6-diamidino-2-phenylindole; blue). Representative images of histologic tumor sections from HCT116 PTEN KO are shown (magnification, ×400).

by LY294002 and showed that changes in tumor [^{18}F]FDG kinetics could be due at least in part to reduced membrane localization of GLUT-1. Thus, [^{18}F]FDG PET could represent a pharmacodynamic biomarker of anti-PI3K pathway treatment. In this context, [^{18}F]FDG PET reports on the modulation of target activity rather that downstream changes in cell viability that is often associated with the use of [^{18}F]FDG PET [40–42]. We did not evaluate long-term/short-term drug effects on [^{18}F]FDG PET as LY294002 has poor pharmacokinetics and is therefore unsuitable for chronic dosing [43–45]. Notably, the reduction in tumor glucose metabolism after LY294002 treatment occurred in both PTEN WT/KO xenografts, that is, drug-induced changes in glucose metabolism were independent of the PTEN expression status. This observation further supports our suggestion that glucose metabolism is probably sufficiently activated in WT cells despite the low activated AKT protein expression and, by extension, that p-AKT protein expression *per se* may be an inappropriate marker of cognate pathway effects on glucose metabolism.

We conclude that [^{18}F]FDG PET is a suitable pharmacodynamic biomarker of PI3K inhibition independent of *PTEN* status.

Acknowledgments

The authors thank B. Vogelstein (Sidney Kimmel Comprehensive Cancer Center, John Hopkins University School of Medicine, Baltimore, MD) for donating of the isogenic set of cells HCT116 PIK3CA WT/MUT.

References

[1] Engelman JA (2009). Targeting PI3K signalling in cancer: opportunities, challenges and limitations. *Nat Rev Cancer* **9**, 550–562.

[2] Cully M, You H, Levine AJ, and Mak TW (2006). Beyond PTEN mutations: the PI3K pathway as an integrator of multiple inputs during tumorigenesis. *Nat Rev Cancer* **6**, 184–192.

[3] Li J, Yen C, Liaw D, Podsypanina K, Bose S, Wang SI, Puc J, Miliaresis C, Rodgers L, McCombie R, et al. (1997). PTEN, a putative protein tyrosine phosphatase gene mutated in human brain, breast, and prostate cancer. *Science* **275**, 1943–1947.

[4] Steck PA, Pershouse MA, Jasser SA, Yung WK, Lin H, Ligon AH, Langford LA, Baumgard ML, Hattier T, Davis T, et al. (1997). Identification of a candidate tumour suppressor gene, *MMAC1*, at chromosome 10q23.3 that is mutated in multiple advanced cancers. *Nat Genet* **15**, 356–362.

[5] Cantley LC and Neel BG (1999). New insights into tumor suppression: PTEN suppresses tumor formation by restraining the phosphoinositide 3-kinase/AKT pathway. *Proc Natl Acad Sci USA* **96**, 4240–4245.

[6] Kandel ES, Skeen J, Majewski N, Di Cristofano A, Pandolfi PP, Feliciano CS, Gartel A, and Hay N (2002). Activation of Akt/protein kinase B overcomes a G(2)/M cell cycle checkpoint induced by DNA damage. *Mol Cell Biol* **22**, 7831–7841.

[7] Liu P, Cheng H, Roberts TM, and Zhao JJ (2009). Targeting the phosphoinositide 3-kinase pathway in cancer. *Nat Rev Drug Discov* **8**, 627–644.

[8] Garcia-Echeverria C and Sellers WR (2008). Drug discovery approaches targeting the PI3K/Akt pathway in cancer. *Oncogene* **27**, 5511–5526.

[9] Nguyen Q-D and Aboagye EO (2010). Imaging the life and death of tumors in living subjects: preclinical PET imaging of proliferation and apoptosis. *Integr Biol* **2**, 483–495.

[10] Macheda ML, Rogers S, and Best JD (2005). Molecular and cellular regulation of glucose transporter (GLUT) proteins in cancer. *J Cell Physiol* **202**, 654–662.

[11] Bentley J, Itchayanan D, Barnes K, McIntosh E, Tang X, Downes CP, Holman GD, Whetton AD, Owen-Lynch PJ, and Baldwin SA (2003). Interleukin-3–

mediated cell survival signals include phosphatidylinositol 3-kinase–dependent translocation of the glucose transporter GLUT1 to the cell surface. *J Biol Chem* **278**, 39337–39348.

[12] Buerkle A and Weber WA (2008). Imaging of tumor glucose utilization with positron emission tomography. *Cancer Metastasis Rev* **27**, 545–554.

[13] Elstrom RL, Bauer DE, Buzzai M, Karnauskas R, Harris MH, Plas DR, Zhuang H, Cinalli RM, Alavi A, Rudin CM, et al. (2004). Akt stimulates aerobic glycolysis in cancer cells. *Cancer Res* **64**, 3892–3899.

[14] Gottlob K, Majewski N, Kennedy S, Kandel E, Robey RB, and Hay N (2001). Inhibition of early apoptotic events by Akt/PKB is dependent on the first committed step of glycolysis and mitochondrial hexokinase. *Genes Dev* **15**, 1406–1418.

[15] Majumder PK, Febbo PG, Bikoff R, Berger R, Xue Q, McMahon LM, Manola J, Brugarolas J, McDonnell TJ, Golub TR, et al. (2004). mTOR inhibition reverses Akt-dependent prostate intraepithelial neoplasia through regulation of apoptotic and HIF-1–dependent pathways. *Nat Med* **10**, 594–601.

[16] Plas DR, Talapatra S, Edinger AL, Rathmell JC, and Thompson CB (2001). Akt and Bcl-xL promote growth factor–independent survival through distinct effects on mitochondrial physiology. *J Biol Chem* **276**, 12041–12048.

[17] Plas DR and Thompson CB (2005). Akt-dependent transformation: there is more to growth than just surviving. *Oncogene* **24**, 7435–7442.

[18] Lee C, Kim JS, and Waldman T (2004). *PTEN* gene targeting reveals a radiation-induced size checkpoint in human cancer cells. *Cancer Res* **64**, 6906–6914.

[19] Samuels Y, Diaz LA Jr, Schmidt-Kittler O, Cummins JM, Delong L, Cheong I, Rago C, Huso DL, Lengauer C, Kinzler KW, et al. (2005). Mutant *PIK3CA* promotes cell growth and invasion of human cancer cells. *Cancer Cell* **7**, 561–573.

[20] Workman P, Aboagye EO, Balkwill F, Balmain A, Bruder G, Chaplin DJ, Double JA, Everitt J, Farningham DA, Glennie MJ, et al. (2010). Guidelines for the welfare and use of animals in cancer research. *Br J Cancer* **102**, 1555–1577.

[21] Blanco-Aparicio C, Renner O, Leal JF, and Carnero A (2007). PTEN, more than the AKT pathway. *Carcinogenesis* **28**, 1379–1386.

[22] Downward J (2004). PI 3-kinase, Akt and cell survival. *Semin Cell Dev Biol* **15**, 177–182.

[23] Stiles B, Gilman V, Khanzenzon N, Lesche R, Li A, Qiao R, Liu X, and Wu H (2002). Essential role of AKT-1/protein kinase Bα in PTEN-controlled tumorigenesis. *Mol Cell Biol* **22**, 3842–3851.

[24] Blanco-Aparicio C, Perez-Gallego L, Pequeno B, Leal JF, Renner O, and Carnero A (2007). Mice expressing myrAKT1 in the mammary gland develop carcinogen-induced ER-positive mammary tumors that mimic human breast cancer. *Carcinogenesis* **28**, 584–594.

[25] Hutchinson J, Jin J, Cardiff RD, Woodgett JR, and Muller WJ (2001). Activation of Akt (protein kinase B) in mammary epithelium provides a critical cell survival signal required for tumor progression. *Mol Cell Biol* **21**, 2203–2212.

[26] Lauring J, Cosgrove DP, Fontana S, Gustin JP, Konishi H, Abukhdeir AM, Garay JP, Mohseni M, Wang GM, Higgins MJ, et al. (2010). Knock in of the AKT1 E17K mutation in human breast epithelial cells does not recapitulate oncogenic *PIK3CA* mutations. *Oncogene* **29**, 2337–2345.

[27] Chen Z, Trotman LC, Shaffer D, Lin HK, Dotan ZA, Niki M, Koutcher JA, Scher HI, Ludwig T, Gerald W, et al. (2005). Crucial role of p53-dependent cellular senescence in suppression of Pten-deficient tumorigenesis. *Nature* **436**, 725–730.

[28] Kim JS, Lee C, Bonifant CL, Ressom H, and Waldman T (2007). Activation of p53-dependent growth suppression in human cells by mutations in *PTEN* or *PIK3CA*. *Mol Cell Biol* **27**, 662–677.

[29] Majumder PK, Grisanzio C, O'Connell F, Barry M, Brito JM, Xu Q, Guney I, Berger R, Herman P, Bikoff R, et al. (2008). A prostatic intraepithelial neoplasia–dependent $p27^{Kip1}$ checkpoint induces senescence and inhibits cell proliferation and cancer progression. *Cancer Cell* **14**, 146–155.

[30] Tennant DA, Duran RV, and Gottlieb E (2010). Targeting metabolic transformation for cancer therapy. *Nat Rev Cancer* **10**, 267–277.

[31] Vander Heiden MG, Cantley LC, and Thompson CB (2009). Understanding the Warburg effect: the metabolic requirements of cell proliferation. *Science* **324**, 1029–1033.

[32] Yap TA, Garrett MD, Walton MI, Raynaud F, de Bono JS, and Workman P (2008). Targeting the PI3K-AKT-mTOR pathway: progress, pitfalls, and promises. *Curr Opin Pharmacol* **8**, 393–412.

[33] Vlahos CJ, Matter WF, Hui KY, and Brown RF (1994). A specific inhibitor of phosphatidylinositol 3-kinase, 2-(4-morpholinyl)-8-phenyl-4*H*-1-benzopyran-4-one (LY294002). *J Biol Chem* **269**, 5241–5248.

[34] Bleeker FE, Felicioni L, Buttitta F, Lamba S, Cardone L, Rodolfo M, Scarpa A, Leenstra S, Frattini M, Barbareschi M, et al. (2008). AKT1(E17K) in human solid tumours. *Oncogene* **27**, 5648–5650.

[35] Abubaker J, Bavi PP, Al-Harbi S, Siraj AK, Al-Dayel F, Uddin S, and Al-Kuraya K (2007). *PIK3CA* mutations are mutually exclusive with *PTEN* loss in diffuse large B-cell lymphoma. *Leukemia* **21**, 2368–2370.

[36] Saal LH, Holm K, Maurer M, Memeo L, Su T, Wang X, Yu JS, Malmstrom PO, Mansukhani M, Enoksson J, et al. (2005). *PIK3CA* mutations correlate with hormone receptors, node metastasis, and *ERBB2*, and are mutually exclusive with *PTEN* loss in human breast carcinoma. *Cancer Res* **65**, 2554–2559.

[37] Perez-Tenorio G, Alkhori L, Olsson B, Waltersson MA, Nordenskjold B, Rutqvist LE, Skoog L, and Stal O (2007). *PIK3CA* mutations and *PTEN* loss correlate with similar prognostic factors and are not mutually exclusive in breast cancer. *Clin Cancer Res* **13**, 3577–3584.

[38] Stemke-Hale K, Gonzalez-Angulo AM, Lluch A, Neve RM, Kuo WL, Davies M, Carey M, Hu Z, Guan Y, Sahin A, et al. (2008). An integrative genomic and proteomic analysis of *PIK3CA*, *PTEN*, and *AKT* mutations in breast cancer. *Cancer Res* **68**, 6084–6091.

[39] Blanco-Aparicio C, Canamero M, Cecilia Y, Pequeno B, Renner O, Ferrer I, and Carnero A (2010). Exploring the gain of function contribution of AKT to mammary tumorigenesis in mouse models. *PLoS One* **5**, e9305.

[40] Brepoels L, De Saint-Hubert M, Stroobants S, Verhoef G, Balzarini J, Mortelmans L, and Mottaghy FM (2010). Dose-response relationship in cyclophosphamide-treated B-cell lymphoma xenografts monitored with [18F]FDG PET. *Eur J Nucl Med Mol Imaging* **37**, 1688–1695.

[41] Higashi K, Clavo AC, and Wahl RL (1993). Does FDG uptake measure proliferative activity of human cancer cells? *In vitro* comparison with DNA flow cytometry and tritiated thymidine uptake. *J Nucl Med* **34**, 414–419.

[42] Young H, Baum R, Cremerius U, Herholz K, Hoekstra O, Lammertsma AA, Pruim J, and Price P (1999). Measurement of clinical and subclinical tumour response using [18F]-fluorodeoxyglucose and positron emission tomography: review and 1999 EORTC recommendations. European Organization for Research and Treatment of Cancer (EORTC) PET Study Group. *Eur J Cancer* **35**, 1773–1782.

[43] Davies SP, Reddy H, Caivano M, and Cohen P (2000). Specificity and mechanism of action of some commonly used protein kinase inhibitors. *Biochem J* **351**, 95–105.

[44] Gharbi SI, Zvelebil MJ, Shuttleworth SJ, Hancox T, Saghir N, Timms JF, and Waterfield MD (2007). Exploring the specificity of the PI3K family inhibitor LY294002. *Biochem J* **404**, 15–21.

[45] Guillard S, Clarke PA, Te Poele R, Mohri Z, Bjerke L, Valenti M, Raynaud F, Eccles SA, and Workman P (2009). Molecular pharmacology of phosphatidylinositol 3-kinase inhibition in human glioma. *Cell Cycle* **8**, 443–453.